



HAL
open science

Morphological and genetic analyses reveal a cryptic species complex in the echinoid *Echinocardium cordatum* and rule out a stabilizing selection explanation.

Emilie Egea, Bruno David, Thérèse Choné, Bernard Laurin, Jean-Pierre Féral,
Anne Chenuil

► To cite this version:

Emilie Egea, Bruno David, Thérèse Choné, Bernard Laurin, Jean-Pierre Féral, et al.. Morphological and genetic analyses reveal a cryptic species complex in the echinoid *Echinocardium cordatum* and rule out a stabilizing selection explanation.. *Molecular Phylogenetics and Evolution*, 2016, 94 (Pt A), pp.207-220. 10.1016/j.ympev.2015.07.023 . hal-01205849

HAL Id: hal-01205849

<https://hal.science/hal-01205849>

Submitted on 21 Mar 2019

HAL is a multi-disciplinary open access archive for the deposit and dissemination of scientific research documents, whether they are published or not. The documents may come from teaching and research institutions in France or abroad, or from public or private research centers.

L'archive ouverte pluridisciplinaire **HAL**, est destinée au dépôt et à la diffusion de documents scientifiques de niveau recherche, publiés ou non, émanant des établissements d'enseignement et de recherche français ou étrangers, des laboratoires publics ou privés.

Morphological and genetic analyses reveal a cryptic species complex in the echinoid *Echinocardium cordatum* and rule out a stabilizing selection explanation

E. Egea^a, B. David^b, T. Choné^b, B. Laurin^b, J.P. Féral^a, A. Chenuil^a

^aInstitut Méditerranéen de Biodiversité et d'Ecologie marine et continentale (IMBE), Aix Marseille Université, CNRS, IRD, Avignon Université, Station Marine d'Endoume, Chemin de la Batterie des Lions, 13007 Marseille, France

^bBiogéosciences, UMR CNRS 6282, Université de Bourgogne, 6, bd. Gabriel, 21000 Dijon, France

ABSTRACT

Preliminary analyses revealed the presence of at least five mitochondrial clades within the widespread sea urchin *Echinocardium cordatum* (Spatangoida). In this study, we analyzed the genetic (two mitochondrial and two nuclear sequence loci) and morphological characteristics (20 indices) from worldwide samples of this taxon to establish the species limits, morphological diversity and differentiation. Co-occurring spatangoid species were also analyzed with mitochondrial DNA. The nuclear sequences confirm that mitochondrial lineages correspond to true genetic entities and reveal that two clades (named A and B1) hybridize in their sympatry area, although a more closely related pair of clades (B1 and B2), whose distributions widely overlap, does not display hybridization. The morphology of all *E. cordatum* clade pairs was significantly differentiated, but no morphological diagnostic character was evidenced. By contrast, other spatangoid species pairs that diverged more recently than the *E. cordatum* clades display clear diagnostic characters. Morphological diversity thus appears responsible for the absence of diagnostic characters, ruling out stabilizing selection, a classical explanation for cryptic species. Alternative classical explanations are (i) environmental plasticity or (ii) a high diversity of genes determining morphology, maintained by varying environmental conditions. We suggest a new hypothesis that the observed morphological diversity is selectively neutral and reflects high effective population sizes in the *E. cordatum* complex. It is supported by the higher abundance of this taxon compared with other taxa, a trend for the genetic and morphological diversity to be correlated in Europe, and the higher genetic and morphological diversities found in clades of *E. cordatum* (except B1) than in other spatangoid samples in Europe. However, the Pacific clades do not confirm these trends.

1. Introduction

Cryptic species cover a wide taxonomic spectrum (Knowlton, 1993, 2000; Klautau et al., 1999; Bickford et al., 2007; Pfenninger and Schwenk, 2007; Trontelj and Fišer, 2009), and are being discovered at an increasing rate. Nevertheless, few studies go beyond the raw identification, and even fewer propose hypotheses for the processes involved in cryptic speciation.

When the absence of diagnostic character is established, it may result from the fact that divergence is too recent or from a particular slowdown of morphological differentiation. Comparisons with taxa that are phylogenetically closely related to the cryptic species

complex, for which divergence times are known, (Poore and Andreakis, 2011) can be used to disentangle the two above-mentioned hypotheses.

The most invoked adaptive process to explain crypticism (when recent speciation is ruled out) is stabilizing selection (Eldredge and Gould, 1972; Charlesworth et al., 1982; Colborn et al., 2001; Wiens and Graham, 2005; Caputi et al., 2007; Smith et al., 2011). Stabilizing selection is mostly expected for ecological specialists or taxa displaying restricted distribution ranges. Additionally, morphological conservatism may also result from developmental constraints (Wake et al., 1983; Maynard Smith et al., 1985). In such cases, low morphological variation is expected within each species.

Conversely, crypticism may also be frequent when morphological variation within species is high because the establishment of diagnostic differences among such species takes more time. High polymorphism is expected to be advantageous in environments

submitted to spatio-temporal fluctuations. Morphological polymorphism may be achieved by two different mechanisms: environmental plasticity (a single genotype may lead to a variety of morphologies) or genetic polymorphism. The regime of environmental fluctuations and the life history traits of the taxon play a major role in determining whether plasticity or high genetic diversity is the best strategy (Stearns, 1992). Genetic polymorphism has a cost (the selective load), but it may be sustainable in species with large fecundity and effective population sizes. Whatever the underlying determinism (plasticity or genetic polymorphism), high morphological variability is more likely for taxa with large geographical ranges inhabiting a wide variety of environments. This is the case of species with high dispersal potential.

Although the causes examined above directly involved natural selection, population genetics theory suggests that strictly neutral processes could also be involved. Higher polymorphism at neutral loci is expected for taxa with larger effective population sizes. If such a taxon splits into separate species, ancestral polymorphism will remain shared among the daughter species for a longer time than in taxa with lower effective population sizes. If the phenotypic characteristics studied to diagnose species are selectively neutral (Bijlsma et al., 1991; Ouborg et al., 1991), this leads to an absence of diagnostic characteristics for a longer time in the high effective population size taxon.

Marine benthic organisms with a pelagic phase in their life-cycle are good candidates to investigate factors explaining cryptic species. They are prone to dispersal and may undergo high environmental variations during early development stages, but they are also closely linked to a specific environment once settled on or in the bottom (as juveniles and adults). They are also expected to display large effective population sizes (Boissin et al., 2011; Foltz et al., 2003, 2004). These features may promote different paths toward cryptic speciation: (1) stabilizing selection, (2) diversifying selection or selection for plasticity and (3) large effective population sizes leading to high diversity and thus absence of diagnostic characteristics.

Echinocardium is a genus of the Loveniidae family (order Spatangoida) composed of five contemporaneous species: *E. mediterraneum* Forbes, 1844 in the Mediterranean Sea and on the southern coasts of Portugal and Northern coasts of Morocco; *E. flavescens* Müller, 1776 in the Atlantic Ocean from the southern coasts of Iceland to the Azores; *E. pennatifidum* Norman, 1868 from Norway to Spain; *E. capense* Mortensen, 1907 in the Mediterranean Sea, Japan and Southern Africa (but see Mironov, 2006) and *E. cordatum* Pennant, 1777 presenting an antitropical distribution covering European Seas, from Norway to Greece, the Pacific Ocean in the Northern (Sea of Japan) and Southern hemisphere (Australia and New Zealand), and the Southern Atlantic Ocean (Southern Africa). In addition to these five well-established species, six other forms have long been considered as distinct species, [*E. mortenseni* Thiéry, 1909, *E. laevigaster* Agassiz, 1869, *E. lymani* Lambert & Thiéry, 1917, *E. fenauxi* Péquignat, 1963, *E. australe* Gray, 1851 and *E. zealandicum* Gray, 1851], but their specific status has since been invalidated (Mortensen, 1951; Higgins, 1974; David and Laurin, 1996; Féral et al., 1998).

Echinocardium cordatum occupies temperate sandy to muddy habitats, ranging from the intertidal to more than 250 m deep, but it is absent from American coasts (both Atlantic and Pacific) (Mortensen, 1951; Buchanan, 1963, 1966; Higgins, 1974; Féral et al., 1998; Kashenko, 2007). Its abundance and efficient burrowing activity make it a key ecological species (Osinga et al., 1995; Lohrer et al., 2004, 2005), which can represent up to 60% of the macrobenthic biomass (Nakamura, 2001). *E. cordatum* has a benthopelagic life cycle with external fertilization leading to a pelagic planktotrophic larva that settles and metamorphoses into a benthic juvenile. The echinopluteus larva can stay between 15

and 40 days into the water column (Kashenko, 2007; Nunes and Jangoux, 2007). During the first 12 days, the larvae remain distant from the bottom and can, in theory, drift over large distances (Shanks et al., 2003; Shanks, 2009) potentially contributing to genetic homogeneity. *E. cordatum* is probably the most studied Spatangoid, for its general biology (Moore, 1935, 1936; Goodwin and Srisukh, 1951; Buchanan, 1966; Duineveld and Jenness, 1984; De Ridder et al., 1985; Yakovlev, 1987; De Ridder and Jangoux, 1993; Osinga et al., 1995; Nunes and Jangoux, 2004; Vopel et al., 2007; Egea et al., 2011), ecology (Thatje et al., 1999; Dautov, 2000; Rosenberg et al., 2002; Ozolin'sh and Nekrasova, 2003; Lohrer et al., 2004, 2005; Gilbert et al., 2007; Zhou et al., 2007; Dashfield et al., 2008; Egea et al., 2011), development (David and Laurin, 1991; Saucedo et al., 2006; Kashenko, 2007; Nunes and Jangoux, 2007), morphology (Higgins, 1974; De Ridder et al., 1987; Ghyoot et al., 1987; David et al., 1988, 1999; Hanot et al., 1990; David and Laurin, 1996) and genetics (Féral et al., 1995, 1998; Chenuil and Féral, 2003; Chenuil et al., 2008). Nevertheless our understanding of the evolutionary history of this taxon remains incomplete.

E. cordatum has long been considered a cosmopolitan species; its broad distribution is consistent with its reproduction mode, although the other species of the genus, which have similar life cycles, are only recorded in European waters (except *E. capense*). Preliminary analyses based on the 16S ribosomal gene of the mitochondrial DNA revealed that *E. cordatum* is split into several mitochondrial lineages. Three lineages were identified in Europe (clade A on the Atlantic coasts, clade B1 in the Mediterranean Sea and the Atlantic coasts of the Iberian Peninsula, and clade B2 in the Mediterranean Sea (Chenuil and Féral, 2003)).

Although molecular approaches, particularly mitochondrial DNA, have proved useful in species delimitation ((Avisé, 2000; Hebert et al., 2003; Vogler and Monaghan, 2007; Meier, 2008) but see also (Galtier et al., 2009)), the occurrence of a deep divergence between mitochondrial lineages does not prove that they are distinct non-interbreeding species because demographic (e.g. a bottleneck) and/or selective events (e.g. several selective sweeps) can generate such topologies within a single panmictic unit (Wakeley, 2006).

The aims of the present study were to confirm whether mitochondrial clades uncovered in *E. cordatum* by Chenuil and Féral (2003) represent true cryptic species and whether they hybridize. We used both mitochondrial and nuclear markers, combined with a large morphological survey. We compared the genetic and morphological diversity, putting the results in perspective with more or less closely related spatangoid species presenting wide distributions and comparable ecologies. Our hypothesis that morphological diversity could be neutral in *E. cordatum* and that large effective population sizes may be associated with a type of cryptic species will be discussed.

2. Material and methods

2.1. Specimen collection & study strategy

The samples studied in this paper were mostly collected by scuba-diving, allowing morphological identification of the specimens according to Mortensen's (1951) identification key. The sampled sites cover most of the European coastline (Fig. 1) and a wide spectrum of environments, from fine silty-sandy (eg. Bodø) to coarse sediment (eg. Marseille).

For the purposes of our study, we considered mitochondrial, nuclear and morphological markers at different scales. First, at the widest geographical and taxonomic scale, mitochondrial 16S and COI sequences were obtained from several *E. cordatum*

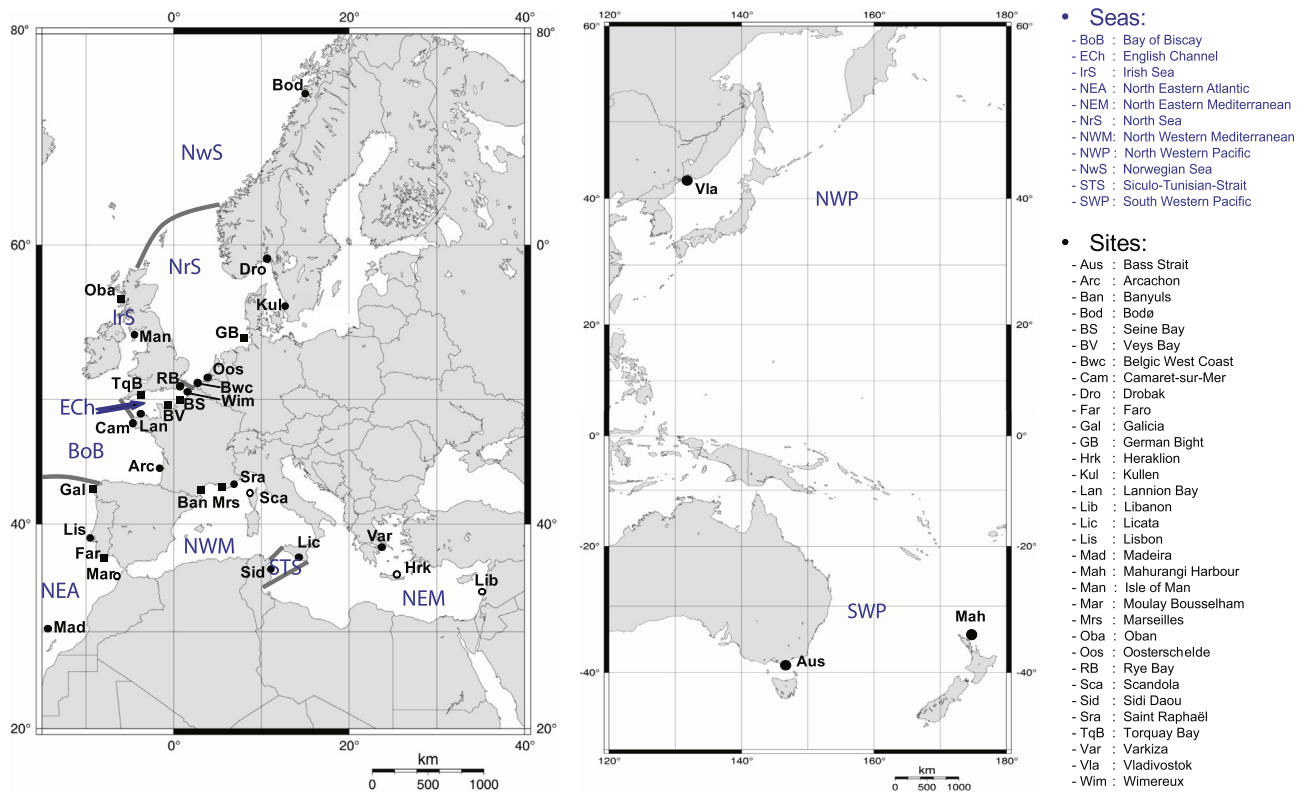


Fig. 1. Geographic localization of *Echinocardium* sampling sites. Solid black squares indicate localities for which several closely sites were sampled. Circles indicate unique sampling site. Solid black symbols represent localities where *E. cordatum* was sampled, whereas empty symbols indicate presence of other species of *Echinocardium* but not *E. cordatum*.

populations, as well as from other species of the genus: *E. mediterraneum*, *E. capense*, *E. flavescens* and *E. pennatifidum*, and from a set of species phylogenetically more or less closely related and presenting comparable distribution areas and habitats, such as other Loveniidae, the Spatangidae *Spatangus purpureus* and the Schizasteridae of the genus *Abatus* (Table 1). Nuclear markers were then characterized in the different mitochondrial clades of *E. cordatum* to test whether gene flow was restricted among them. Third, because morphology provides valuable diagnostic characteristics to differentiate species of the genus *Echinocardium* (Laurin et al.,

1994; David and Laurin, 1996; David et al., 1999), we performed an analysis of the morphology within *E. cordatum* and searched for morphological significant differences between the mitochondrial clades.

2.2. Molecular analyses

DNA was extracted from the spines or gonads preserved in 95% ethanol using the Chelex® 100 chelating resin (Sigma) (Walsh et al., 1991) as described in Chenuil and Féral (2003).

Table 1

Number of individuals/haplotypes sequenced for each genetic marker or analyzed for 20 morphological indices, according to mitochondrial clades (determined by 16S nucleotide sequence) or origin (gray cells). For nuclear loci, several sequences were done per individual after PCR-cloning.

Taxon\marker	Mt-16S	Mt-COI	Nuc-EF1	Nuc-i21	Morphometric indices
Main goal	Determine mitochondrial clade in large samples	Add precision to mitochondrial clades phylogeny	Assess whether mitochondrial lineages exchange genes		Characterize morphological diversity and differentiation
<i>Echinocardium cordatum</i> (all)	678/99	33/33	221	289	522
Clade A	245/37	9/9	88	112	96
Clade B1	197/17	6/6	68	85	195
Clade B2	197/41	14/14	39	44	81
Clade NP	20/3	2/2	10	25	22
Clade SP	19/7	2/2	15	23	128
<i>Echinocardium mediterraneum</i>	164/38	2/2	0	0	a
<i>Echinocardium capense</i>	14/5	0	0	0	a
<i>Echinocardium flavescens</i>	9/2	2/2	0	0	a
<i>Echinocardium pennatifidum</i>	16/5	1	0	0	a
<i>Spatangus purpureus</i>	15/5	1	0	0	0
<i>Abatus nimrodi</i>	1	1	0	0	0
<i>Abatus cavernosus</i>	5/4	1	0	0	0
<i>Abatus shackletoni</i>	1	1	0	0	0
<i>Brissopsis lyrifera</i>	5/4	1	0	0	0

* Some morphological analyses were performed by some authors of this study (David et al., 1999) but were not included here.

The 16S ribosomal gene and a portion of the *Cytochrome Oxidase subunit 1 (COI)* of the mitochondrial genome were amplified for various individuals of the five *Echinocardium* species and for *S. purpureus* (Table S1), as in Chenuil et al. (2008), for 16S with 16SF2 (5'GTTTCGCCTGTTTACCAAAAACAT) and 16SR (5'CGAACAGACCAACCC TTTAAAAGC) primers and for the partial COI gene using Stockley et al. (2005) COIe5 (5'GCYTGAGCWGGCA TGGTAGG) and COIe3 (5'GCTCGTGCRCTACRTCCAT) primers. For these two markers, PCR reactions were performed in 25 μ l final volume using 1 μ l of the DNA solution, with 0.65 U of the GoTaq[®] Flexi DNA Polymerase 5 u/ μ l (Promega), 5 μ l of the 5X Colorless GoTaq[®] Flexi Buffers, 1.55 μ M of MgCl₂, both provided by the manufacturer, 0.2 mM of each dNTP and 0.9 μ M of each primer. Amplification was performed on a 96 well Eppendorf Mastercycler[®]. For the 16S marker, an initial denaturation step at 94 °C for 3 min was followed by 40 cycles of three steps: 94 °C for 40 s, annealing at 65 °C for 30 s and elongation at 72 °C for 2 min. For COI, a similar program was used, except that the initial denaturation step was followed by 35 cycles of 30 s at 94 °C, 30 s at 52 °C and 1 min at 72 °C, followed by a final elongation at 72 °C for 5 min.

Exon Primed Intron Crossing (EPIC) provides fast evolving nuclear markers potentially applicable across species and for which evolutionary relationships among alleles can be inferred (Chenuil et al., 2010). To study the nuclear genome, two markers were obtained for *E. cordatum* based on Chenuil et al. (2010): the first intron of the Elongation Factor 1 α (EF1 α) and the intron of the Calpain gene (i21). These markers were, respectively, amplified with specifically designed primers EF1 α -F (5'TAGTTGGTTTCAATA TCAAGAACG), and EF1 α -R (5'AATATGAGCAGTATGGCAATCCA), and i21-F (5'GGAGATAGTCGTCTATGATGAC), and i21-R (5' GTTGA TCCAGAGGATGACATGTA). For these markers, the PCR reactions were performed in 13 μ l final volumes using 1 μ l of the DNA solution, with 0.35 U of the GoTaq[®] Flexi DNA Polymerase 5 u/ μ l (Promega), 1.3 μ l of the 5X Colorless GoTaq[®] Flexi Buffers, 0.5 μ M of MgCl₂, 0.2 mM of each dNTP and 1.5 μ M of each primer. For EF1 α , the PCR amplification program was composed of an initial denaturation step at 94 °C for 2 min followed by 40 cycles of 94 °C for 30 s, 55 °C for 1 min and 72 °C for 1 min 30 s and a final elongation step of 3 min at 72 °C. For i21, only 35 cycles of 20 s at 94 °C, 1 min at 57 °C and 1 min at 72 °C were performed, followed by 5 min at 72 °C.

Cloning of the nuclear markers was performed using the pGEM[®]-T Easy Vector Systems (Promega) according to manufacturers' recommendations. Positive clones were screened for the presence of appropriate-sized inserts by PCR amplifications, and clones (when possible, four per individual) were sequenced using the T7 universal primer (5'-TAATACGACTCACTATAGGG-3). PCR products for mitochondrial markers were sequenced with the primers 16SR2 and COIe3. Cloning PCR products can create artefactual mutations leading to more than two allelic forms for a diploid organism (Bierne et al., 2007). For both i21 and EF1 α , a proportion of approximately 80% of the individuals displayed, after cloning their PCR product, more than two different sequences. When more than two different sequences were obtained for the same individual, those presenting 99% similarity were considered as PCR artifact products of the same allele (Acinas et al., 2005; Schloss et al., 2011). The "true" allele was then considered as the consensus of the different sequences, the spurious sequences were identified by the fact that they were in low frequency (singletons in each individual cloning) and very similar to more frequent haplotypes (that may be frequent also in the global sample, i.e. the whole clade) (Bierne et al., 2007).

Once the alleles were defined, intron sequences were aligned using MUSCLE (Edgar, 2004) in the Seaview platform (Galtier

et al., 1996) and using the ClustalW algorithm (Thompson et al., 1994) in BioEdit for the mitochondrial markers.

Phylogenetic tree reconstructions were conducted for each marker. Maximum likelihood analysis was performed with PhyML 3.0 (Guindon et al., 2010). All parameters of the nucleotide substitution model and the gamma shape parameter were simultaneously estimated by maximum likelihood and were adjusted. A batch bootstrap procedure was applied (1000 replicates). Bayesian analyses were performed using MrBayes 3.2 (Huelsenbeck and Bollback, 2001; Ronquist and Huelsenbeck, 2003) and with 3,000,000 iterations, the first 10% being considered as the burn in.

The best substitution model implemented in MrBayes 3.2 and PhyML 3.0 was determined for each marker, according to the Bayesian Information Criterion (BIC) (Schwarz, 1978; Posada and Buckley, 2004) using jModelTest 0.1.1 (Posada, 2008).

The information contained in indels can be treated in different ways. Aside from considering gaps as a fifth state and multi-position gaps as separate presence/absence characteristics, gaps can be considered as missing data or can be coded to consider multi-position gaps as a single mutational event (simple indel coding or multiple indel coding method (Simmons and Ochoterena, 2000; Müller, 2005a, 2005b)). For introns, all four indel coding strategies were compared in order to determine the best coding procedure to extract the maximum information from gaps.

Genetic diversity was estimated with DnaSP 5.10.11 software (Rozas et al., 2003), for 16S, EF1 α and i21 but not for COI for which the sample size was too low. Rarefaction analysis (Mousadik and Petit, 1996) was performed at the 16S locus using Contrib (Petit et al., 1998) to correct for large sample size differences between species.

Haplotype or allele networks were reconstructed with the program Network 4.5.1.0 (www.fluxus-engineering.com) using the Median-Joining method (Bandelt et al., 1999).

The hierarchical structure of the genetic variation of the nuclear data sets was examined by Analysis of MOlecular VAriance (AMOVA) as implemented in Arlequin software (Excoffier et al., 1992; Excoffier and Lischer, 2010). The components of genetic variance were computed at two hierarchical levels: between mitochondrial clades (σ^2_a), and among geographical areas within those clades (σ^2_b). Differentiation between samples was assessed by computing pairwise F_{ST} and Φ_{ST} with Arlequin software. F_{ST} was calculated using Slatkin's distance, and Φ_{ST} was based on the pairwise difference between alleles. Significance was assessed using 1000 permutations.

The genealogical Sorting Index (gsi) (Cummings et al., 2008) measures the degree of genealogical divergence in a specified group of taxa supplementing the bootstrap support and the posterior probability of monophyly by providing an independent measure of monophyly on a scale between zero and one. The null hypothesis that the degree of monophyly observed is what would be expected at random is tested through permutations, and a rejection of the null hypotheses implies that the labelled groups are distinct from each other. A high GSI indicates substantial sorting of ancestral polymorphisms and implies low gene flow between groups. Gsi analyses were conducted using the web interface (www.genealogicalsortingindex.org) for each tested locus based on 100 randomly sampled Bayesian posterior distributions of trees and tested via 10,000 permutations. These 100 individual GSI measurements were then used together with equal weight to calculate an ensemble GSI statistic (gsiT) for each locus. Thus, GSI_T measurements serve as a summary of the genealogical exclusivity across the Bayesian posterior distribution of trees for a given locus and monophyly is considered to be supported when the gsi_T values are above 0.90 and are significant at $P < 0.001$ (Cummings et al., 2008).

2.3. Morphological analyses

Morphometric analyses were conducted on 522 individuals of the five clades of *Echinocardium cordatum* coming from different locations (Tables 1 and S2) and various environments. Only adult specimens over 20 mm long were retained for analysis to reduce allometric effects (David and Laurin, 1991). Before measurement, the tests of the specimens were cleaned of their appendages following Higgins's Method (1974). The morphology of each specimen was characterized via 21 morphometric parameters combined into 20 indices (David and Laurin, 1991; David et al., 1999). These parameters cover the most important aspects of the morphology of sea urchins: general shape, fascioles, architecture of plastron and ambulacral areas (David et al., 1999, Fig. S1). Multivariate analyses were performed in two steps. A principal component analysis (PCA) was conducted without *a priori* information on the mitochondrial clade of individuals, and the discriminant analysis (DA) was performed after assignment of each individual to its mitochondrial clade. The mitochondrial clade was determined for each specimen according to the 16S gene sequence or, for Pacific samples for which we could not access DNA, according to geographical location (Table S2). ANOVA and non-parametric tests were also used to test the differences found by PCA and DA. The Mahalanobis distance (Mardia et al., 1979) was used to quantify the morphological distance between clades.

3. Results

3.1. Mitochondrial DNA

A total of 668 individuals of *Echinocardium cordatum* were sequenced for the mt-16S marker, allowing for determination of their mitochondrial clade. More than 200 specimens of co-occurring spatangoids (mostly from genus *Echinocardium*) were also sequenced for this marker (Table 1). To determine the phylogenetic relationships among clades and *Echinocardium* species, 33 *E. cordatum* and 5 other *Echinocardium* samples were also sequenced for mt-COI (Table 1). The 16S ribosomal gene alignment (446 bp) revealed a greater genetic diversity of the nominal species *E. cordatum* compared to the other species of the genus *Echinocardium* or to *S. purpureus* (Table 2: Poly, H, Hd). The rarefaction analysis set to the lowest number of individuals considered for a single species (i.e. $N = 9$) confirmed this result (Table 2: A_R). The nucleotide diversity π was also higher for *E. cordatum*, with a ten-fold difference between *E. cordatum* and *E. mediterraneum*.

This higher genetic diversity can be explained by the phylogenetic tree (Fig. 2 right panel) obtained from the 16S marker with the best fitted model Hasegawa–Kishino–Yano (HKY) model (Hasegawa et al., 1985) and gamma-shaped rate variation across sites (HKY + G), showing a deeply structured genetic diversity in *E. cordatum*, with five mitochondrial clades displaying distinct geographic distributions (Fig. 3). Individuals forming clade A were found only in the North Eastern Atlantic Ocean, from the Norway Sea to Lisbon, individuals of clades SP and NP were collected, respectively, in the Southern Pacific Ocean (Australia and New Zealand), and in the Northern Pacific (Vladivostok), and clades B1 and B2 were restricted to the Mediterranean Sea, from Greece to Spain, except for some individuals of clade B1 that were also encountered on the West coast of Iberia (Galicia and South of Portugal).

For COI analyses, the substitution model was determined for each codon position. The most appropriate model implemented in MrBayes 3.2 for the first and second codon position was GTR + G, whereas F81 (Felsenstein, 1981) and equal rates were most appropriate for the third position. For PhyML 3.0 analyses, we selected the best fitted model for the whole molecule: HKY + I + G.

Table 2

Genetic diversity at three markers, mt-16S, intron EF1 α and intron i21, for the five mitochondrial clades of *E. cordatum* and, only for mt-16S, for other sea urchin spatangoid species living in the same environment. N: number of sequences, TNS: total number of sites, for nuclear markers we put the total alignment length, but there are numerous insertions and deletions according to alleles, Poly: number of polymorphic sites, H/A: number of haplotypes or alleles, Hd: haplotypic diversity, Sd Hd: standard deviation of haplotype diversity, A_R : rarefied allelic richness to $N = 9$, and π : nucleotide diversity.

	N	TNS*	Poly	H/A	Hd	Sd Hd	π	A_R9
16S								
<i>E. cordatum</i> (all)	678	429	78	99	0.84	0.012	0.0210	5.3
<i>E. cord.</i> clade A	245	432	38	37	0.49	0.040	0.0016	4.0
<i>E. cord.</i> clade B1	197	441	18	17	0.18	0.038	0.0006	0.9
<i>E. cord.</i> clade B2	197	441	35	41	0.78	0.030	0.0030	4.3
<i>E. cord.</i> clade NP	20	443	2	3	0.28	0.123	0.0007	1.2
<i>E. cord.</i> clade SP	19	442	9	7	0.80	0.063	0.0060	3.8
<i>E. mediterraneum</i>	164	441	36	38	0.64	0.043	0.0020	3.4
<i>E. capense</i>	14	427	5	5	0.51	0.158	0.0020	2.6
<i>E. flavescens</i>	9	446	1	2	0.22	0.166	0.0005	1
<i>E. pennatifidum</i>	16	441	8	5	0.75	0.078	0.0020	2.4
<i>S. purpureus</i>	15	444	4	5	0.64	0.129	0.0017	3.1
EF1α								
<i>E. cordatum</i> (all)	221	602	nd	108	0.94	0.010	0.023	nd
<i>E. cord.</i> clade A	88	602	nd	51	0.92	0.024	0.012	nd
<i>E. cord.</i> clade B1	68	602	nd	36	0.78	0.055	0.022	nd
<i>E. cord.</i> clade B2	39	602	nd	35	0.99	0.008	0.029	nd
<i>E. cord.</i> clade NP	10	602	nd	2	0.20	0.024	0.001	nd
<i>E. cord.</i> clade SP	15	602	nd	4	0.60	0.113	0.015	nd
i21								
<i>E. cordatum</i> (all)	289	420	nd	56	0.70	0.029	0.024	nd
<i>E. cord.</i> clade A	112	420	nd	51	0.91	0.023	0.024	nd
<i>E. cord.</i> clade B1	85	420	nd	37	0.78	0.049	0.016	nd
<i>E. cord.</i> clade B2	44	420	nd	39	0.99	0.001	0.040	nd
<i>E. cord.</i> clade NP	25	420	nd	12	0.88	0.050	0.029	nd
<i>E. cord.</i> clade SP	23	420	nd	9	0.68	0.105	0.011	nd

The COI tree (not shown) was mostly concordant with the genetic structure observed with the 16S locus: clade A was still opposed to a super clade comprising B1, B2, SP and NP, but in contrast to the 16S tree, clades SP and NP clustered together in a monophyletic group (clade P) in the same way as B1 and B2, although the posterior probability of this node was low (0.88).

Genetic distances (K2P) among *E. cordatum* clades ranged from 1.35% to 3.86% for 16S and from 2.31% to 8.58% for COI (Table S3). In contrast, the 16S within-clade genetic distances never exceeded 0.30% (Table S3, diagonal). For the 16S marker, the haplotype diversity varied among clades, and B1 displayed a lower diversity compared to the two other European clades (for which the sampling effort is comparable).

The best supported topology (for the relationships among *E. cordatum* clades and *Echinocardium* species) was obtained with the concatenated data set joining the two mitochondrial markers (16S and COI), with the best model of evolution corresponding to each portion, as specified above. The Bayesian (MrBayes) and maximum likelihood (PhyML) topologies were identical. This topology was the same as the COI topology, with higher node supports, although support for the NP + SP clade (Fig. 2 left panel) was still modest (0.66 posterior probability for MrBayes, and 60% bootstrap for the PhyML tree). This tree also displays the molecular patristic distances among three species of the genus *Spatangus*, which are well-defined morphologically, and appeared genetically much closer than the distances between clade A and other *E. cordatum* clades.

Contrary to *E. cordatum*, *E. mediterraneum* and *S. purpureus*, which were also present in both the Atlantic Ocean and the Mediterranean Sea, did not exhibit any genetic subdivision, and some 16S haplotypes were shared between the Atlantic and Mediterranean basins (Figs. 2 and S2).

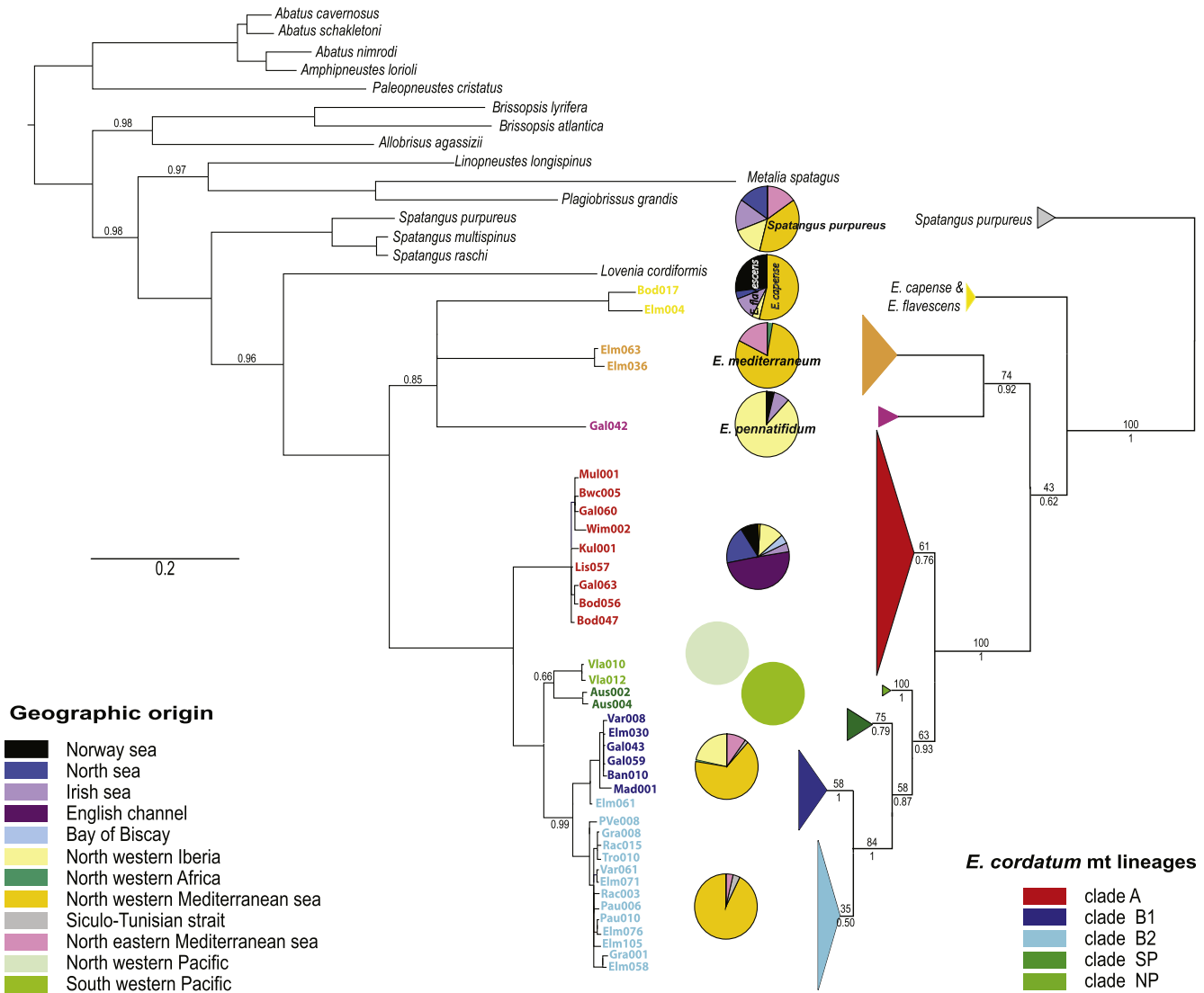


Fig. 2. Left: Bayesian phylogenetic reconstruction of concatenated mt-COI and mt-16S genes. Only posterior probabilities lower than 1 are indicated (1,000,000 iterations). Right: 16S gene phylogenetic reconstruction obtained by the Bayesian and maximum likelihood methods. Posterior probabilities and bootstrap values are given, respectively, under and above each branch of the tree. Central pie charts indicate the geographical origin of individuals analyzed for the 16S marker for each clade, according to the “geographic origin” legend. Color of individual identification codes on the concatenated mt-COI and mt-16S genes correspond to the clade color in Figs. 3 and 4. (For interpretation of the references to color in this figure legend, the reader is referred to the web version of this article.)

3.2. Nuclear genome

Nuclear markers were successfully amplified for the five *E. cordatum* mitochondrial clades, as well as for some individuals of *E. flavescens* (EF1 α and i21) and *E. pennatifidum* (i21).

Although incorporating indel information can provide reliable characters for phylogenetic analysis (Barriel, 1994; Simmons and Ochoterena, 2000; Müller, 2005; Simmons et al., 2007), particularly for introns (Creer, 2007), it was not the case here. Considering gaps as a 5th state, missing data, or recoding indels with the simple indel coding procedure (Simmons and Ochoterena, 2000) gave concordant phylogenetic information. Consequently, in subsequent analyses only alignments considering gaps as missing data are presented.

Both introns displayed a high genetic diversity (Table 2) with a global heterozygosity of 0.94 for EF1 α and 0.70 for i21.

The phylogenetic tree obtained with the HKY + G nucleotide substitution model (not shown) and allelic network reconstruction

of EF1 α (Fig. 4a) highlighted a strong structuring of alleles in good agreement with the formerly identified mitochondrial clades.

Alleles isolated from individuals of mitochondrial clade A tended to cluster together (cluster A) except for a few, mostly from Galicia, which were found in cluster B1 (out of 12 alleles in cluster B1 that are not issued from individuals of the B1 mitochondrial clade, 7 were isolated from Galician samples). Conversely, the A cluster also presented alleles belonging to individuals of other mitochondrial clades (mostly B1, 5 out of 7 alleles). All alleles from the Northern Pacific individuals formed a monophyletic clade, and alleles from New Zealand and Australia clustered in two distinct groups according to their geographic origin. Only two alleles of individuals belonging to the SP mitochondrial clade were not found in this group but within the A and B2 clusters. Clades B1 and B2 were less well-distinguished (numerous alleles of B1 individuals clustering into a dominantly B2 group).

In contrast, the global reconstruction of both the i21 phylogenetic tree (not shown) and allele network showed no apparent

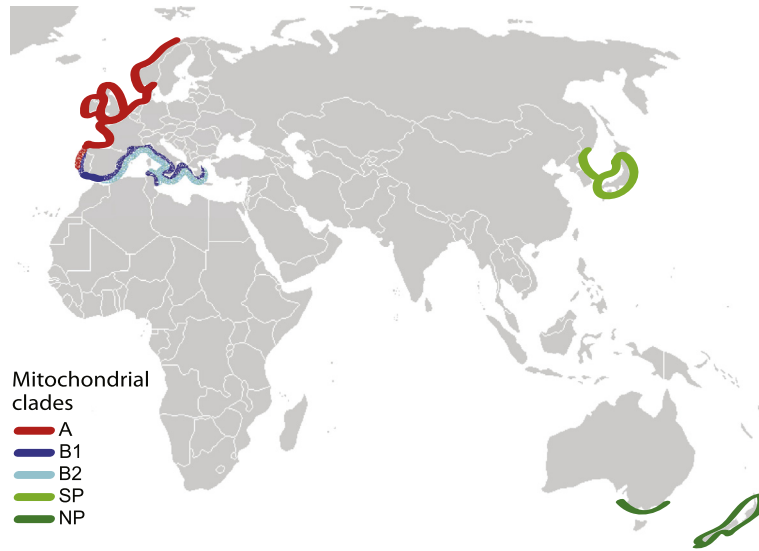


Fig. 3. Confirmed geographic distribution of *E. cordatum* mitochondrial clades.

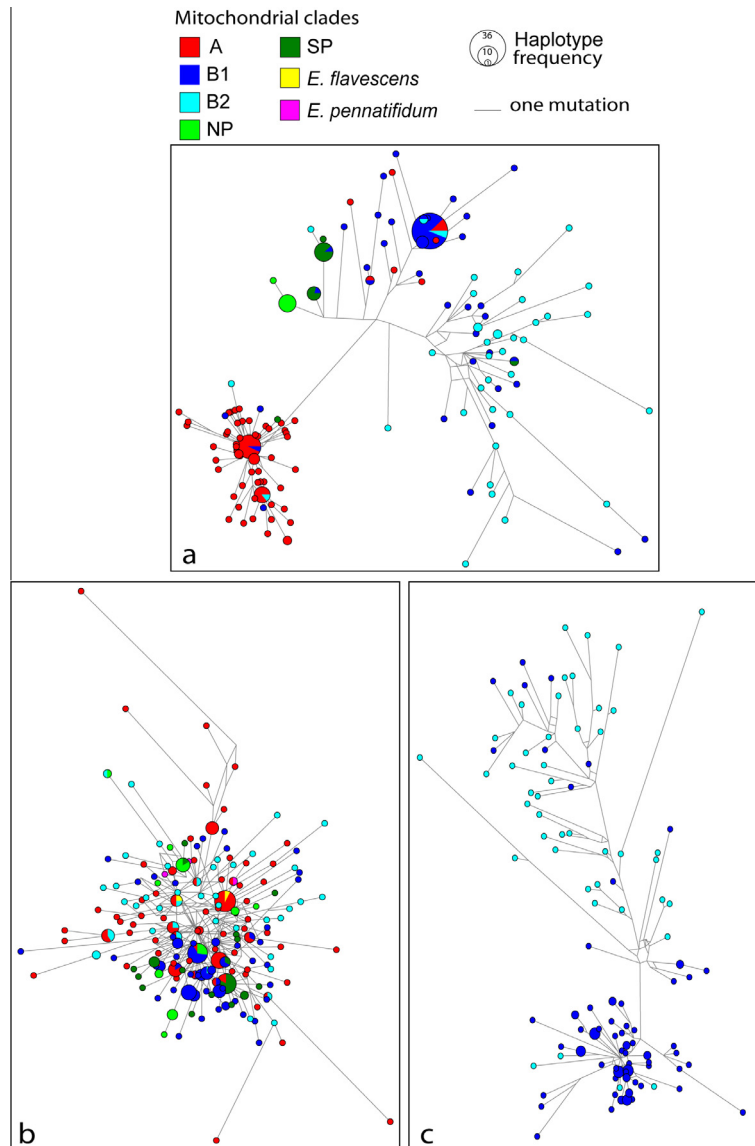


Fig. 4. Allele networks of EF1 α (a) and i21 markers (b and c with only clades B1 & B2) with individual mitochondrial clade assignment.

Table 3

Genetic differentiation Φ_{ST} values and significance ($*p < 0.05$, NS: Not Significant) between pairs of clades found in sympatry for nuclear markers. The number of alleles analyzed for each clade and locus is given in parentheses. For geographic indication, refer to Fig. 1.

	EF1 α	i21
A vs. B1 in Galicia B1	-0.05 NS (A-9/B1-9)	-0.01 NS (A-8/B1-20)
vs. B2 in Marseille B1	0.12 * (B1-17/B2-17)	0.13 (B1-16/B2-21)
vs. B2 in Banyuls B1	0.25* (B1-10/B2-19)	0.13* (B1-13/B2-16)
vs. B2 in Varkiza	0.44* (B1-10/B2-3)	0.17* (B1-18/B2-7)

clustering of alleles by mitochondrial lineage (Fig. 4b) except when the reconstruction was restricted to B1 and B2 (Fig. 4c).

Nevertheless, the analysis of molecular variance (AMOVA) performed on alleles grouped according to their mitochondrial clade and sampling localities concluded that for both EF1 α and i21, a significant part of the total genetic variation could be explained by the belonging of individuals to one mitochondrial clade or another.

Significant Φ_{ST} differences were found for all pairwise comparisons of clades with both EF1 α and i21. When the tests were restricted to localities where two different clades occurred in sympatry, the Φ_{ST} values and related permutation tests revealed significant differentiation between clades B1 and B2, regardless of the locality, whereas clades A and B1 showed no genetic structuring of their nuclear alleles in Galicia (Table 3).

Although the monophyly of mitochondrial clades has not been achieved for the nuclear genes, there was significant (P values < 0.05) genealogical divergence between groups across all loci. GSI analyses of the tree generated from the Bayesian analyses of the EF1 gene and the i21 introns confirmed that all labelled groups were monophyletic with significant measures of exclusive ancestry ($p < 0.05$), even if only low-moderate genealogical divergence was exhibited (the low GSI $_T$ values ranged from 0.19 to 0.50).

3.3. Morphology

The total length of the test reached much larger values for B1 (up to 86.38 mm) compared to all other clades. Nonparametric Dunn's bilateral test, corrected for multiple test comparisons with the Bonferroni procedure confirmed that the test sizes in clade B1 were significantly different than the other four clades. Clade A also showed significant differences from clades B2 and SP (Fig. S3).

This parameter is not a candidate diagnostic character of mitochondrial lineages because young individuals of the "large" clade are in the range of the "small" clades. Numerous morphological indices displayed significant differences among clades (Table S4), but the overlapping distributions (boxplots Fig. S4) forbid their use as diagnostic characters.

The Principal Component Analysis on morphological data highlighted the differences among clades, although some individuals presented intermediate morphologies (Fig. 5). The first three axes represented 49.40% of the total variance. Clade B1 was well-separated from the other clades on the first two axes, except for a pool of specimens from Galicia that mixed with clade A individuals. Individuals of SP and NP formed two groups separated on the second axis, whereas individuals of clades A and B2 were best differentiated on the third axis. Dunn's test on the pairwise differences of the coordinates of individuals on axes F1, F2 and F3 confirmed the statistical differentiation among mitochondrial clades (Fig. 5 bottom).

Morphological differentiation between B1 and B2 was confirmed when individuals of syntopic populations were compared in the PCA (Fig. 6a and b), but no differentiation was found for individuals of clades A and B1 in Galicia, the only region where they were found in sympatry (Fig. 6c).

The discriminant analysis established a model combining the 20 indices to maximize the discrimination of *a priori* defined groups (here the mitochondrial clades). Four axes condensing 100% of the total dataset variance were defined, with the two first axes representing 82.61% of this variance. As in the PCA, individuals of the different mitochondrial clades clustered together (not shown). The reassignment tests allowed, on the basis of the generated model, *a posteriori* reattributing individuals to one or the other groups defined *a priori*. These tests correctly reassigned, on average, 94.64% of the specimens (90.63% for clade A, 90.91% for NP, 93.83% for B1, 94.36% for B2 and 99.22% for SP). When individuals from Galicia were removed, the average global reassignment success increased to 95.84%, with 95.40% correct reassignment for clade A individuals.

The morphological disparity of each clade was estimated by calculating the average distance on the 20 axes (Table 4) between each individual's coordinate projection and the barycenter of the corresponding clade. Despite a higher sample size, clade B1 displayed the lowest disparity, revealing a significantly lower morphological diversity than the other European clades A and B2 as established by Dunn's tests (Table 4).

When the genetic distances estimated by calculating the Φ_{ST} between clades on the 16S marker were compared with the morphological Mahalanobis distances (Table 5) using the mantel test, no correlation between the genetic and morphological distances were highlighted (regression coefficient $R^2 = 0.03$ NS). The genetically closest clades (B1 and B2) were distinct morphologically (based on the PCA in Fig. 5).

4. Discussion

4.1. *Echinocardium cordatum*, a complex of cryptic species

4.1.1. Presence of different species and hybridization

Mitochondrial genetic data (16S and COI) reveal at least five genetic entities in *Echinocardium cordatum*: mitochondrial clades A, B1, B2, SP and NP (Fig. 2) found mostly in allopatry (Fig. 3), except for clades B1 and B2 found in sympatry and even syntopy around the Mediterranean Sea, and clades A and B1, which present a zone of contact on the western coasts of the Iberian Peninsula (Galicia). These results agree with the study of Chenuil and Féral (2003) based on a much smaller sample size. When divergent lineages (reciprocally monophyletic) are allopatrically distributed, vicariance is the most likely interpretation (i.e. a long period of allopatry led to divergent clades, eventually allopatric speciation in case of reproductive isolation). When lineages are found in sympatry however, selective sweeps or bottlenecks are plausible alternative hypotheses to explain the absence of intermediate haplotypes, leading to a pattern of divergent clades (within a single species). Nuclear markers segregating independently of the mitochondrial genome offer an efficient tool to discriminate the species of a complex (Zhang and Hewitt, 2003; Boissin et al., 2008, 2011; Poore and Andreakis, 2011). In theory, if independent molecular markers generate similar topologies and congruent individual clustering patterns, reproductive isolation among lineages is definitely established. However, when clades defined by distinct markers do not perfectly match, this does not rule out the hypothesis of reproductive isolation because it can reflect the historical events responsible for the extant distribution of evolutionary lineages (e.g., Ross et al., 2010). Although the nuclear markers (EF1 α and i21, Fig. 4) show imperfect or no reciprocal monophyly according to mitochondrial clades, the GSI analyses, AMOVA and genetic differentiation statistics (Table 3) confirm the significant differentiation among all pairs of mitochondrial clades at both loci, even in sympatry, (clades B1 and B2, Table 3), demonstrating limited gene flow between these two clades despite the lack of physical barriers. On

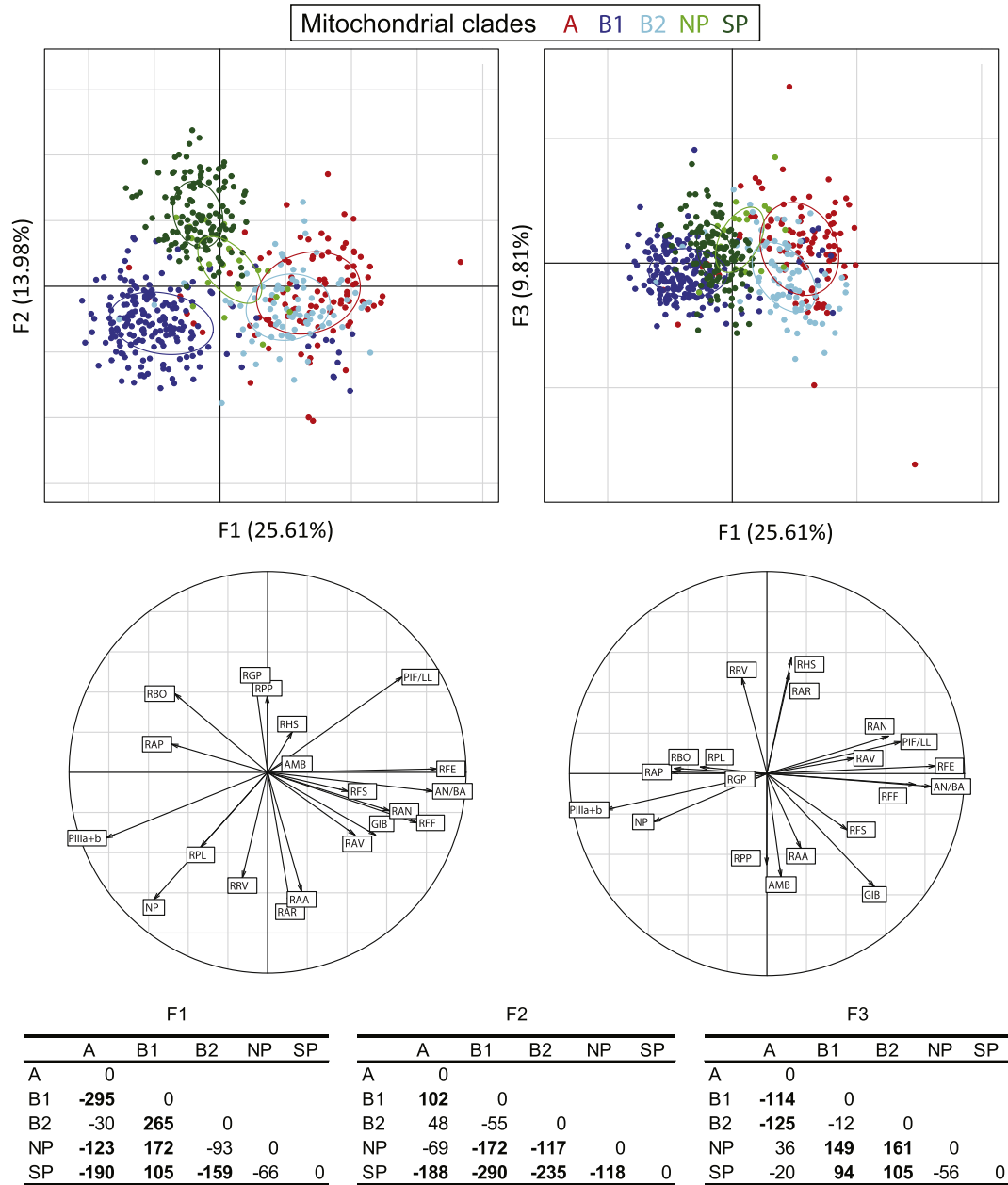


Fig. 5. Top: morphological PCA performed on the 20 morphometric indices considered (indices are coded as in David and Laurin, 1991). Specimens are mapped according to their mitochondrial clades on the first 3 axes; middle: correlation circle quantifying the contribution of indices (arrow lengths) and correlation among indices (arrow angles); bottom: pairwise differences among clades of mean individual coordinate projections on the first 3 axes, bold values indicate significant differences among clades.

the contrary, clades A and B1, which are sympatric in Galicia, show no genetic differentiation of their nuclear alleles in this sample location (Table 3), suggesting contemporaneous gene flow in this area. This results from a secondary contact and cannot be a zone of origin from where two populations (A and B1) diverged because the mitochondrial lineages are very divergent, and no intermediate haplotypes are found in this zone.

Genetic distances between mitochondrial lineages are often used as preliminary indicators to identify candidate species (Vences et al., 2005; Fouquet et al., 2007; Vieites et al., 2009). Here, the COI K2P-distances between mitochondrial clades of *E. cordatum* (2.31–8.58%) are comparable with the levels of inter-specific divergence identified among other complexes of cryptic species (Landry et al., 2003; Hebert et al., 2004; Hart et al., 2006; Wilson et al., 2007; Owen et al., 2009; Stöhr et al., 2009; Puillandre et al., 2010) and between closely related species of echinoderms

(Palumbi, 1996; Wada et al., 1996; McCartney et al., 2000; Lessios et al., 2001; Kerr et al., 2005).

Based on the genetic distances calculated between the mitochondrial clades and on the absence of gene flow between the two closest clades B1 and B2, all mitochondrial clades fulfill the phylogenetic species concept and are characterized by distinct evolutionary trajectories, although the possibility of interbreeding is not excluded (observed gene flow between clades A and B1 in Galicia). Even though this mitochondrial clade revives the spectrum of previously described and then discarded sister/synonymous species of *Echinocardium cordatum*, it is not possible here to assign any of the clades to such species. Considering the significant larger test size of clade B1 specimens, one would be tempted to assign them to *E. fenauxi* which was described as a larger species compared to *E. cordatum* in the second paper of Péquignat (1964), but the fact that the species was founded on a chimera made of

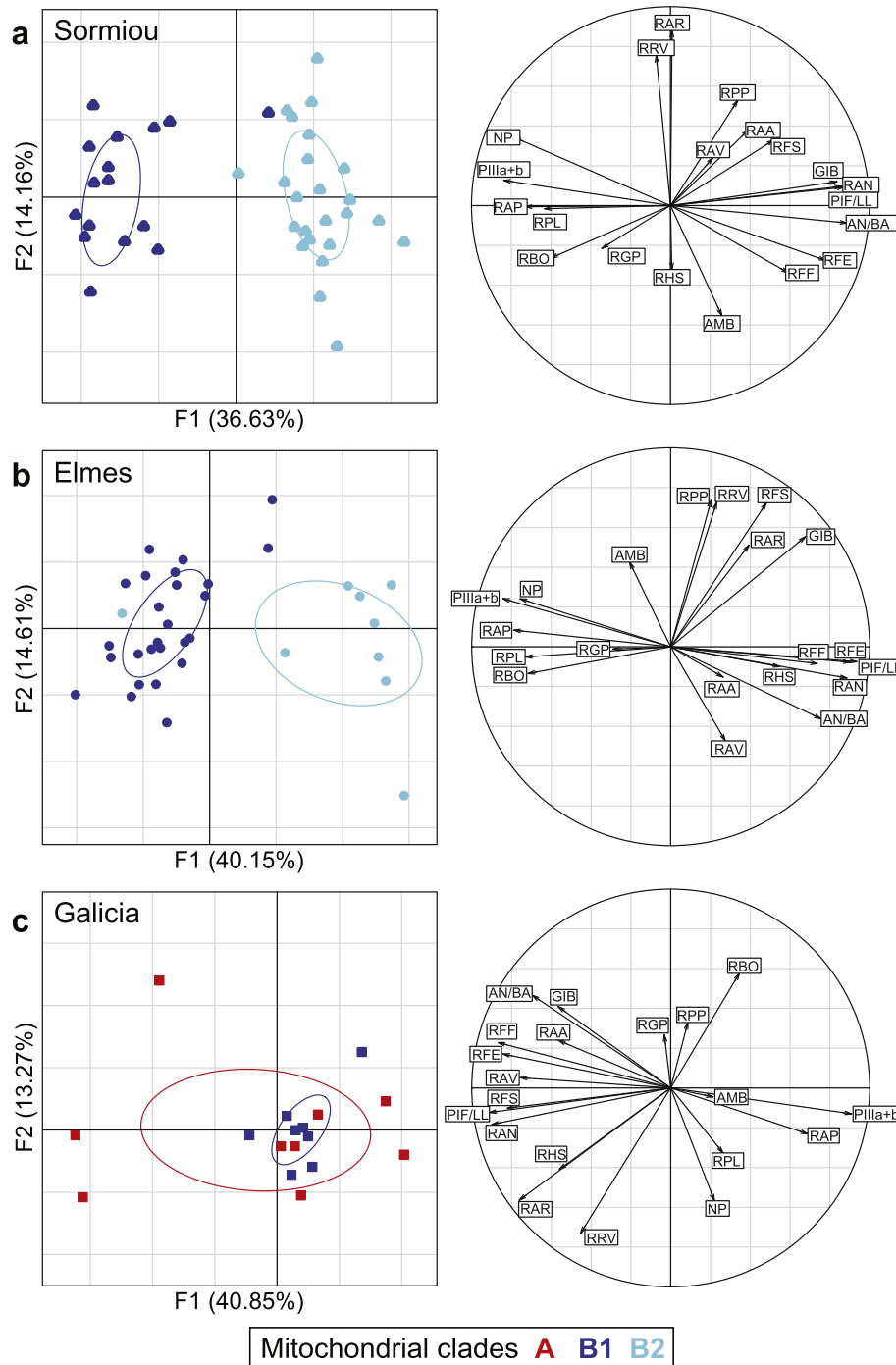


Fig. 6. Morphological PCA from individuals of different clades sampled at the same location (a: Sormiou station at Marseilles, b: Elmes station at Banyuls, c: Galicia station at Galicia see Fig. 1) and contribution of indices.

Table 4

(a) Multidimensional disparity of clades [$\sqrt{(\sum \text{distance-to-barycenter}^2)}$], N Ind: number of individuals of the group; and (b) Dunn's test on morphological disparities among pairs of clades.

	Clade disparity	N Ind		A	B1	B2	NP
<i>a</i>			<i>b</i>				
A	4.164	96	B1	<0.0001*			
B1	3.220	195	B2	0.133	0.005*		
B2	3.493	81	NP	0.644	0.122	1.000	
NP	3.527	22	SP	0.001*	0.112	0.714	0.872
SP	3.304	128					

* Indicates a significant *p*-value after Bonferroni correction.

Table 5

Upper matrix: pairwise Mahalanobis morphological distances; lower matrix: 16S population pairwise ϕ st.

	A	B1	B2	NP	SP
A	0	21.87	15.85	27.16	30.02
B1	0.95	0	18.79	27.88	36.07
B2	0.92	0.90	0	34.69	37.26
NP	0.87	0.98	0.92	0	18.61
SP	0.88	0.97	0.88	0.84	0

fragments from several specimens collected in France and in Italy, and the concomitant absence of morphotype of *E. fenauxi* prevent to re-use this name. Morpho-cladistic studies of clade SP individuals could permit to confirm that the morpho-group S2 identified in David et al., 1999 is in fact *Echinocardium australe*.

4.2. Morphological data confirm the cryptic species status

The morphological study performed on genetically characterized individuals reveals a statistically significant morphological differentiation between the putative cryptic species of the *E. cordatum* species complex (Figs. 5 and 6) with the discriminant analysis correctly reassigning 95.8% of the individuals to their mitochondrial clade. In the principal component analyses, individuals of the sympatric clades B1 and B2 are statistically segregated (Fig. 6a and b), whereas the morphospaces delineated by individuals of clades A and B2 greatly overlap, despite their strictly allopatric distributions. In the same way, individuals of Les Elmes and Sormiou (Fig. 1: NWM: sampling sites of Ban and Mrs respectively) are more efficiently segregated according to their mitochondrial clade (B1 or B2) than according to their locality. One striking exception to this morphological differentiation matching mitochondrial clades is the population of Galicia (Fig. 6c) where individuals from mitochondrial clades A and B1 display considerable morphological variation that covers all of the morphospace between type A and B1, including morphologies distinct from A and B1 from other locations, reflecting an increased variability, likely related to the new multilocus genotypes generated by hybridization.

4.2.1. Comparison with other cases

4.2.1.1. Decoupling of genetic and morphological evolution. Molecular datings based on fossil calibrations from the genus *Echinocardium* and mitochondrial sequences of 16S estimated a divergence time of approximately 6 million years between clade A and clade B (B1 and B2) (Chenuil & Féral, 2003). This datation suggests that morphological differentiation between cryptic species of *Echinocardium cordatum* is particularly slow. Indeed, other well-differentiated echinoid species such as *Eucidaris thouarsii* Agassiz & Desor, 1846 and *E. tribuloides* Lamarck, 1816, diverged “only” 3 million years ago, following the formation of the Isthmus of Panama. Similarly, our phylogenetic tree based on the mitochondrial COI sequences (Fig. 2) also established that a pair of morphologically well-differentiated spatangoid sea urchins (*Spatangus purpureus* and *S. multispinus*) diverged more recently than *E. cordatum*'s mitochondrial clades.

In mussels of the genus *Mytilus*, three nominal species, *M. edulis*, *M. galloprovincialis*, and *M. trossulus*, form well-known hybrid zones in Europe (Bierne et al., 2003; Gardner and Thompson, 2009) and divergence time estimations are of 2 mya between *M. edulis* and *M. galloprovincialis* and of 3.5 mya between *M. trossulus* and the other two species (Hilbish et al., 2000). Analyses of Morphological Mahalanobis distances and overlap in the distribution of individuals on Principal Component Analysis plots reflected a lower morphological differentiation among *Mytilus* species (Gardner and Thompson, 2009) than among *E. cordatum* species (this study), a paradox knowing that *E. cordatum* spp. do not display any diagnostic characters whereas *M. edulis*, *M. galloprovincialis*, and *M. trossulus* constitute nominal species. This supports (cf last section) that it is the very high morphological diversity in *E. cordatum* clades that causes the absence of diagnostic characters, because it leads to character overlap, despite a statistically very significant morphological differentiation. Compared to *E. cordatum*, the morphological differentiation among *Mytilus* species is better correlated to divergence times (Gardner and Thompson, 2009): *M. trossulus*, the first species to have diverged, is much more differentiated morphologically than *M. edulis* and *M. galloprovincialis* are

from one another (Hilbish et al., 2000) although morphology and genetic divergence are far from being proportional in *Mytilus*. In *E. cordatum*, the discrepancy between morphological and genetic divergence is even more salient because the two closest species (B1 and B2, estimated to have diverged about 2 mya) are much more differentiated morphologically than A and B2 (6 mya divergence).

4.2.1.2. Highly divergent species hybridize in *E. cordatum*. Hybridization of *E. cordatum* cryptic species that diverged more than 6 mya (clades A and B1) is exceptional. Indeed, the cryptic species complex of *Ciona intestinalis* is considered remarkable for the divergence time of its cryptic and hybridizing species, although lineages that were shown to hybridize in this complex diverged only about 3 mya (Roux et al., 2013). Numerous cases of hybridizations have been reported in marine benthic invertebrates, some of them occurring in the Northeastern Atlantic Coast of France (e.g. Bierne et al., 2003, for *Mytilus* spp., and Becquet et al., 2012; Strelkov et al., 2007, for *Macoma balthica*) and in Spain, particularly in Galicia where we found *E. cordatum* hybrids (Hurtado et al., 2011, for the groove carpet shell *Ruditapes decussatus* with an introduced *Ruditapes*, see also Conde-Padín et al., 2007; Guerra-Varela et al., 2009). Theory predicts that tension zones, i.e. hybrid zones maintained by counterselection of hybrids, are expected to be trapped in regions where natural barriers to gene flow occur, where population density is lower, or in ecotones, even when counterselection is not caused by different environmental optima but by genomic incompatibilities (Barton, 1979). It is therefore not possible to determine the factors controlling the location of the tension zone in *E. cordatum* from our analysis. Genetic analyses with codominant markers in additional populations of the Atlantic Coasts of Iberia and France are necessary to establish the precise nature of *E. cordatum* hybridization.

4.2.2. Mechanisms leading to cryptic species apparition in *E. cordatum*

The fact that the two phylogenetically closest clades (B1 & B2) display morphologies statistically more different than clades with higher genetic distances suggests a decoupling of the molecular and morphological evolution within the species complex (genetic and morphologic distances are not correlated). Many cases of cryptic speciation are attributed to (i) stabilizing selection (Dobzhansky, 1970; Mayr, 1982), which maintains a constant phenotype across the range of the group (Williamson, 1987) as a result of a strong pressure of the environment or (ii) to fluctuating selection, which leads to the retention of a high morphological polymorphism or to the acquisition of a certain plasticity on a character, both mechanisms preventing the appearance of diagnostic morphological differences between species. Under the stabilizing selection hypothesis, only a limited number of morphologies co-exist in the same environment (Lieberman and Dudgeon, 1996; Colborn et al., 2001; Sáez et al., 2003).

According to this hypothesis, distinct clades of *E. cordatum* found in the same environment should share the same morphologies. On the contrary, our morphological analyses reveal significant morphological differentiation for all pairwise comparisons among clades, even for those living in syntopy in the different sampled areas (Mrs, Ban, Var) (except in Galicia where A and B1 hybridize).

Furthermore, stabilizing selection is not likely to occur in benthopelagic species such as *E. cordatum*, which due to their high dispersal potential, may encounter a wide range of environmental conditions. By contrast, spatio-temporal environmental variation may have two consequences: either the evolution of environmental plasticity or the presence of a high genetic diversity at loci determining adaptation to environmental conditions.

Although never considered, a simpler hypothesis, the selective neutrality of morphological diversity, could account for such

cryptic species with high morphological variability. The high morphological diversity of *E. cordatum*, causing the absence of diagnostic characters, may be a simple consequence of its high effective population size, leading to high genetic diversity of characters encoding morphology. Indeed, *E. cordatum* is the most abundant spatangoid species found when diving or dredging in Europe. European clades A and B2 display higher rarefied allelic richness for the mt-16S marker compared to other species, such as *E. mediterraneum*, *E. pennatifidum*, *E. flavescens*, *E. capense* or *Spatangus purpureus*, living in the same basins (see A₉ Table 2), suggesting a higher effective population size. Another observation supports the hypothesis that the diversity of the morphological characters in *E. cordatum* may simply reflect neutral genetic diversity (thus effective population size): clade B1 displays a much lower genetic diversity than clades A and B2 at all markers (mt-16S, i21 and EF1) and presents a significantly lower morphological disparity (Table 4). This finding suggests that this clade has a lower effective population size than the other clades. Including the Pacific clades in the comparison does not confirm this trend, which may be partly caused by their much lower sample sizes for genetic (NP and SP clades), and morphological data (NP). More detailed genetic and morphological analyses at the level of populations and investigating the correlations among genetic and morphological diversity levels among populations would allow further testing of the hypothesis that morphological diversity is neutral in *E. cordatum*. This will not be straightforward because morphology is very likely influenced by environmental plasticity in *Echinocardium cordatum* and *E. flavescens* (Saucède et al., 2006, and David, pers comm.). If neutral evolution of morphology appeared to be a common phenomenon, cryptic species complexes would be expected to be more frequent in taxa with high effective population sizes. This factor may contribute to the high frequency of marine cryptic species (Knowlton, 1993) because numerous marine species have large fecundities.

Acknowledgments

The authors wish to thank all of the people who provided samples, including Audrey Darnaude, Igor Dolmatov, Franck Gentil, Hermann Hummel, Ingrid Kroencke, Drew Lorher, Xavier de Montaudouin, Gauthier Rollet and Marc Taymour Joly.

We also acknowledge the support of the consortium GBiRM, within the Network of Excellence 'Marine Biodiversity and Ecosystem Functioning' (MarBEF), which was funded by the Sustainable Development, Global Change and Ecosystems Programme of the European Community's Sixth Framework Programme (contract no. GOCE-CT- 2003-505446). Additional support for the molecular work was obtained from the network Marine Genomics Europe (GOCE-CT-2004-505403). The authors also want to thank Abigail Cahill for english revision of parts of the manuscript.

Appendix A. Supplementary material

Supplementary data associated with this article can be found, in the online version, at <http://dx.doi.org/10.1016/j.ympcv.2015.07.023>.

References

Acinas, S.G., Sarma-Rupavtarm, R., Klepac-Ceraj, V., Polz, M.F., 2005. PCR-induced sequence artifacts and bias: insights from comparison of two 16S rRNA clone libraries constructed from the same sample. *Appl. Environ. Microbiol.* 71 (12), 8966–8969.

Avise, J., 2000. *Phylogeography: The History and Formation of Species*. Harvard Univ Pr.

Bandelt, H., Forster, P., Röhl, A., 1999. Median-joining networks for inferring intraspecific phylogenies. *Mol. Biol. Evol.* 16 (1), 37.

Barriel, V., 1994. Phylogénies moléculaires et insertions-délétions de nucléotides = Molecular phylogenies and how to code insertion/deletion events. *Comptes rendus de l'Académie des sciences. Série 3, Sciences de la vie* 317 (7), 693–701.

Barton, N., 1979. The dynamics of hybrid zone. *Heredity* 43, 341–359.

Becquet, V., Simon-Bouhet, B., Pante, E., Hummel, H., Garcia, P., 2012. Glacial refugium versus range limit: conservation genetics of *Macoma balthica*, a key species in the Bay of Biscay (France). *J. Exp. Mar. Biol. Ecol.* 432–433, 73–82.

Bickford, D., Lohman, D.J., Sodhi, N.S., Ng, P.K.L., Meier, R., Winker, K., Ingram, K.K., Das, I., 2007. Cryptic species as a window on diversity and conservation. *Trends Ecol. Evol.* 22 (3), 148–155.

Bierne, N., Borsa, P., Daguin, C., Jollivet, D., Viard, F., Bonhomme, F., David, P., 2003. Introgression patterns in the mosaic hybrid zone between *Mytilus edulis* and *M. galloprovincialis*. *Mol. Ecol.* 12, 447–461.

Bierne, N., Tanguy, A., Faure, M., Faure, B., David, E., Boutet, I., Boon, E., Quere, N., Plouviez, S., Kemppainen, P., Jollivet, D., Moraga, D., Boudry, P., David, P., 2007. Mark-recapture cloning: a straightforward and cost-effective cloning method for population genetics of single-copy nuclear DNA sequences in diploids. *Mol. Ecol. Notes* 7 (4), 562–566.

Bijlsma, R., Ouborg, N., Treuren, R., Seitz, A., Loeschcke, V., 1991. Genetic and phenotypic variation in relation to population size in two plant species: *Salvia pratensis* and *Scabiosa columbaria*. *Spec. Conserv. Populat.-Biolog. App.*, 89–101.

Boissin, E., Féral, J.P., Chenuil, A., 2008. Defining reproductively isolated units in a cryptic and syntopic species complex using mitochondrial and nuclear markers: the brooding brittle star, *Amphipholis squamata* (Ophiuroidea). *Mol. Ecol.* 17 (7), 1732–1744.

Boissin, E., Stohr, S., Chenuil, A., 2011. Did vicariance and adaptation drive cryptic speciation and evolution of brooding in *Ophioderma longicauda* (Echinodermata: Ophiuroidea), a common Atlanto-Mediterranean ophiuroid? *Mol. Ecol.* 20 (22), 4737–4755.

Buchanan, J.B., 1963. The bottom fauna communities and their sediment relationships off the coast of Northumberland. *Oikos* 14, 154–175.

Buchanan, J.B., 1966. The biology of *Echinocardium cordatum* (Echinodermata: Spatangoidea) from different habitats. *J. Mar. Biol. Assoc. UK* 46, 97–114.

Caputi, L., Andreakis, N., Mastrototaro, F., Cirino, P., Vassillo, M., Sordino, P., 2007. Cryptic speciation in a model invertebrate chordate. *Proc. Natl. Acad. Sci.* 104 (22), 9364–9369.

Charlesworth, B., Lande, R., Slatkin, M., 1982. A neo-Darwinian commentary on macroevolution. *Evolution* 36 (3), 474–498.

Chenuil, A., Egea, E., Rocher, C., Touzet, H., Féral, J.P., 2008. Does hybridization increase evolutionary rate? Data from the 28S-rDNA D8 domain in echinoderms. *J. Mol. Evol.* 67 (5), 539–550.

Chenuil, A., Féral, J.P., 2003. Sequences of mitochondrial DNA suggest that *Echinocardium cordatum* is a complex of several sympatric or hybridizing species. A pilot study. *Echinoderm Research 2001*. In: *Proc. 6th Eur. Conf. Echinoderm, Banyuls-sur-mer, France*. J.-P. Féral and B. David. Lisse, NL, Swets & Zeitlinger Publishers, pp. 15–21.

Chenuil, A., Hoareau, T., Egea, E., Penant, G., Rocher, C., Aurelle, D., Mokhtar-Jamai, K., Bishop, J., Boissin, E., Diaz, A., Krakau, M., Luttkhuizen, P., Patti, F., Blavet, N., Mousset, S., 2010. An efficient method to find potentially universal population genetic markers, applied to metazoans. *BMC Evol. Biol.* 10 (1), 276.

Colborn, J., Crabtree, R.E., Shaklee, J.B., Pfeiler, E., Bowen, B.W., 2001. The evolutionary enigma of Bonefishes (*Albula* spp.): cryptic species and ancient separations in a globally distributed shorefish. *Evolution* 55 (4), 807–820.

Creer, S., 2007. Choosing and Using Introns in Molecular Phylogenetics. *Evolution. Bioinform.*, 2007 (EBO-3-Creer-et-al).

Conde-Padín, P., Carvajal-Rodríguez, A., Carballo, M., Caballero, A., Rolán-Alvarez, E., 2007. Genetic variation for shell traits in a direct-developing marine snail involved in a putative sympatric ecological speciation process. *Evol. Ecol.* 21, 635–650.

Cummings, M.P., Neel, M.C., Shaw, K.L., Otto, S., 2008. A genealogical approach to quantifying lineage divergence. *Evolution* 62 (9), 2411–2422.

Dashfield, S.L., Somerfield, P.J., Widdicombe, S., Austen, M.C., Nimmo, M., 2008. Impacts of ocean acidification and burrowing urchins on within-sediment pH profiles and subtidal nematode communities. *J. Exp. Mar. Biol. Ecol.* 365 (1), 46–52.

Dautov, S., 2000. Distribution, species composition, and dynamics of echinoderm larvae in an area of the Tumen River Estuary and of the Far East State Marine Reserve. *Russ. J. Mar. Biol.* 26 (1), 12–17.

David, B., Laurin, B., 1991. The elaborate ontogeny of the spatangoid echinoid *Echinocardium cordatum*: a test of the standards of heterochronic trajectories. *Geobios* 24 (5), 569–583.

David, B., Laurin, B., 1996. Morphometrics and cladistics: measuring phylogeny in the sea urchin *Echinocardium*. *Evolution* 50 (1), 348–359.

David, B., Laurin, B., Choné, T., Magniez, F., 1999. Morphological disparity in the genus *Echinocardium* (Echinoidea: Spatangoidea). In: *Candia Carnevali, M.-D., Bonasoro, F. (Eds.), Echinoderm Research Conference, 1998, Milan, Italy*. Rotterdam, Balkema, pp. 253–259.

David, B., Laurin, B., De Ridder, C., 1988. How *Echinocardium cordatum* (Pennant) shows sexual dimorphism. In: *Burke, R.D., Mladenov, P.V., Lambert, P., Parsley, R.L. (Eds.), Sixth Intern. Echinoderm Conference, Victoria, Rotterdam, Balkema*.

De Ridder, C., Jangoux, M., 1993. The digestive tract of the spatangoid echinoid *Echinocardium cordatum* (Echinodermata): morphofunctional study. *Acta Zoologica* 74, 337–351.

De Ridder, C., Jangoux, M., Van Impe, E., 1985. Food selection and absorption efficiency in the spatangoid echinoid *Echinocardium cordatum* (Echinodermata). In: *Proc. 5th Internat. Echinoderm Conf., Galway, A.A. Balkema, Rotterdam*.

- De Ridder, C., Jangoux, M., De Vos, L., 1987. Frontal ambulacral and peribuccal areas of the spatangoid echinoid *Echinocardium cordatum* (Echinodermata): a functional entity in feeding mechanism. *Mar. Biol.* 94 (4), 613–624.
- Dobzhansky, T., 1970. *Genetics of the Evolutionary Process*. Columbia Univ. Press, New York.
- Duineveld, G.C.A., Jenness, M.I., 1984. Differences in growth rate of the sea urchin *Echinocardium cordatum* as estimated by the parameter omega of the Vvon Bertalanffy equation applied to skeletal rings. *Mar. Ecol. Prog. Ser.* 19, 65–72.
- Edgar, R.C., 2004. MUSCLE: multiple sequence alignment with high accuracy and high throughput. *Nucleic Acids Res.* 32 (5), 1792–1797.
- Egea, E., Mérigot, B., Mahé-Bézac, C., Féral, J.-P., Chenuil, A., 2011. Differential reproductive timing in *Echinocardium* spp.: the first Mediterranean survey allows interoceanic and interspecific comparisons. *C.R. Biol.* 334 (1), 13–23.
- Eldredge, N., Gould, S.J., 1972. Punctuated equilibria: an alternative to phyletic gradualism. *Models Paleobiol.* 82, 115.
- Excoffier, L., Lischer, H., 2010. Arlequin suite ver 3.5: a new series of programs to perform population genetics analyses under Linux and Windows. *Molecul. Ecol. Resour.* 10 (3), 564–567.
- Excoffier, L., Smouse, P.E., Quattro, J.M., 1992. Analysis of molecular variance inferred from metric distances among DNA haplotypes: application to human mitochondrial DNA. *Genetics* 131, 479–491.
- Felsenstein, J., 1981. Evolutionary trees from DNA sequences: a maximum likelihood approach. *J. Mol. Evol.* 17 (6), 368–376.
- Féral, J.P., Poulin, E., Derelle, E., Gallardo, S., Chambon, C., 1995. Genetic differentiation of *Echinocardium cordatum* as revealed by allozymes and RNA sequencing. In: Emson, R., Smith, A., Campbell, A. (Eds.), *Echinoderm Research Conference, 1995*, London, UK. Rotterdam, Balkema.
- Féral, J.P., Poulin, E., Oubelkheir, K., 1998. Geographic and genetic differentiation of *Echinocardium cordatum* (Pennant) – the current state of a complex question: the status of *Echinocardium fenaxi* (Péquignat). In: Mooler, R., Telford, M. (Eds.), *Echinoderms Conference 1996*, San Francisco. Rotterdam, Balkema, pp. 647–649.
- Foltz, D.W., 2003. Invertebrate species with nonpelagic larvae have elevated levels of nonsynonymous substitutions and reduced nucleotide diversities. *J. Mol. Evol.* 57, 607–612.
- Foltz, D.W., Hrinkevich, A., Rocha-Olivares, A., 2004. Apparent selection intensity for the cytochrome oxidase subunit I gene varies with mode of reproduction in echinoderms. *Genetica* 122, 115–125.
- Fouquet, A., Vences, M., Salducci, M.-D., Meyer, A., Marty, C., Blanc, M., Gilles, A., 2007. Revealing cryptic diversity using molecular phylogenetics and phylogeography in frogs of the *Scinax ruber* and *Rhinella margaritifera* species groups. *Mol. Phylogenet. Evol.* 43 (2), 567–582.
- Galtier, N., Gouy, M., Gautier, C., 1996. SEAVIEW and PHYLO_WIN: two graphic tools for sequence alignment and molecular phylogeny. *CABIOS* 12 (6), 543–548.
- Galtier, N., Nabholz, B., Glemin, S., Hurst, G.D., 2009. Mitochondrial DNA as a marker of molecular diversity: a reappraisal. *Mol. Ecol.* 18 (22), 4541–4550.
- Gardner, J.P., Thompson, R.J., 2009. Influence of genotype and geography on shell shape and morphometric trait variation among North Atlantic blue mussel (*Mytilus* spp.) populations. *Biol. J. Linn. Soc.* 96, 875–897.
- Ghyoot, M., De Ridder, C., Jangoux, M., 1987. Fine structure and presumed functions of the pedicellariae of *Echinocardium cordatum* (Echinodermata, Echinoidea). *Zoomorphology* 106, 279–288.
- Gilbert, F., Hulth, S., Grossi, V., Poggiale, J.-C., Desrosiers, G., Rosenberg, R., Gérino, M., François-Carcaillet, F., Michaud, E., Stora, G., 2007. Sediment reworking by marine benthic species from the Gullmar Fjord (Western Sweden): importance of faunal biovolume. *J. Exp. Mar. Biol. Ecol.* 348 (1–2), 133–144.
- Goodwin, T.W., Srisukh, S., 1951. Carotenoids in the heart urchin; *Echinocardium cordatum*. *Nature* 167 (4244), 358–359.
- Guerra-Varela, J., Colson, I., Backeljau, T., Breugelmans, K., Hughes, R.N., Rolán-Alvarez, E., 2009. The evolutionary mechanism maintaining shell shape and molecular differentiation between two ecotypes of the dogwhelk *Nuccella lapillus*. *Evol. Ecol.* 23, 261–280.
- Guindon, S., Dufayard, J.F., Lefort, V., Anisimova, M., Hordijk, W., Gascuel, O., 2010. New algorithms and methods to estimate maximum-likelihood phylogenies: assessing the performance of PhyML 3.0. *Syst. Biol.* 59 (3), 307.
- Hanot, P., De Ridder, C., J. M., 1990. Morphologie fonctionnelle des clavules chez le spatangide *Echinocardium cordatum* (Echinoidea, Echinodermata). *Echinoderm Research*.
- Hart, M.W., Keever, C.C., Dartnall, A.J., Byrne, M., 2006. Morphological and genetic variation indicate cryptic species within Lamarck's little sea star, *Parvulastra (=Patriella) exigua*. *Biol. Bull.* 210 (2), 158–167.
- Hasegawa, M., Kishino, K., Yano, T., 1985. Dating the human-ape splitting by a molecular clock of mitochondrial DNA. *J. Mol. Evol.* 22, 160–174.
- Hebert, P.D.N., Penton, E.H., Burns, J.M., Janzen, D.H., Hallwachs, W., 2004. Ten species in one: DNA barcoding reveals cryptic species in the neotropical skipper butterfly *Astrartes fulgerator*. *Proc. Natl. Acad. Sci. USA* 101 (41), 14812–14817.
- Hebert, P.D.N., Ratnasingham, S., de Waard, J.R., 2003. Barcoding animal life: cytochrome c oxidase subunit 1 divergences among closely related species. *Proc. R. Soc. Lond. B Biol. Sci.* 270 (Suppl 1), S96–S99.
- Higgins, R.C., 1974. Specific status of *Echinocardium cordatum*, *E. australe* and *E. zelandicum* (Echinoidea: Spatangoida) around New Zealand, with comments of the relations of morphological variations to environment. *J. Zool. London* 173, 451–475.
- Hilbish, T.J., Mullinax, A., Dolven, S.I., Meyer, A., Koehn, R.K., Rawson, P.D., 2000. Origin of the antitropical distribution pattern in marine mussels (*Mytilus* spp.): routes and timing of transequatorial migration. *Mar. Biol.* 136, 69–77.
- Huelsenbeck, J., Bollback, J., 2001. Application of the likelihood function in phylogenetic analysis. *Handbook of Statistical Genetics*, 415–443.
- Hurtado, N.S., Pérez-García, C., Morán, P., Pantanes, J.J., 2011. Genetic and cytological evidence of hybridization between native *Ruditapes decussatus* and introduced *Ruditapes philippinarum* (Mollusca, Bivalvia, Veneridae) in NW Spain. *Aquaculture* 311, 123–128.
- Kashenko, S., 2007. Adaptive responses of embryos and larvae of the heart-shaped sea urchin *Echinocardium cordatum* to temperature and salinity changes. *Russ. J. Mar. Biol.* 33 (6), 381–390.
- Kerr, A.M., Janies, D.A., Clouse, R.M., Samyn, Y., Kuzsak, J., Kim, J., 2005. Molecular phylogeny of coral-reef sea cucumbers (Holothuriidae: Aspidochirotida) based on 16S mitochondrial ribosomal DNA sequence. *Mar. Biotechnol.* 7 (1), 53–60.
- Klautau, M., Russo, C.A.M., Lazoski, C., Boury-Esnault, N., THorpe, J.P., Solé-Cava, A.M., 1999. Does cosmopolitanism result from overconservative systematics? A case study using the marine sponge *Chondrilla nucula*. *Evolution* 53 (5), 1414–1422.
- Knowlton, N., 1993. Sibling species in the sea. *Annu. Rev. Ecol. Syst.* 24, 189–216.
- Knowlton, N., 2000. Molecular genetic analyses of species boundaries in the sea. *Hydrobiologia* 420, 73–90.
- Landry, C., Geyer, L.B., Arakaki, Y., Uehara, T., Palumbi, S.R., 2003. Recent speciation in the Indo-West Pacific: rapid evolution of gamete recognition and sperm morphology in cryptic species of sea urchin. *Proc. Roy. Soc. Lond. – Biol.* 270 (1526), 1839–1847.
- Laurin, B., David, B., Féral, J.-P., Derelle, E., 1994. Polytypism in the spatangoid sea urchin *Echinocardium*: a morphological vs molecular approach. In: David, B., Guille, A., Féral, J.-P., Roux (Eds.), *Echinoderms Through Time, 1993*, Djion, France. Rotterdam, Balkema, pp. 739–745.
- Lessios, H.A., Kessing, B.D., Pearse, J.S., 2001. Population structure and speciation in tropical seas: global phylogeography of the sea urchin *Diadema*. *Evolution* 55 (5), 955–975.
- Lieberman, B.S., Dudgeon, S., 1996. An evaluation of stabilizing selection as a mechanism for stasis. *Palaeogeogr. Palaeoclimatol. Palaeoecol.* 127 (1–4), 229–238.
- Lohrer, A.M., Thrush, S.F., Gibbs, M.M., 2004. Bioturbators enhance complex biogeochemical interactions. *Nature* 431, 1092–1095.
- Lohrer, A.M., Thrush, S.F., Hunt, L., Hancock, N., Lundquist, C., 2005. Rapid reworking of subtidal sediments by burrowing spatangoid urchins. *J. Exp. Mar. Biol. Ecol.* 321, 155–169.
- Mardia, K.V., Kent, J.T., Bibby, J.M., 1979. *Multivariate Analysis*. Academic Press, London.
- Maynard Smith, J., Burian, R., Kauffman, S., Alberch, P., Campbell, J., Goodwin, B., Lande, R., Raup, D., Wolpert, L., 1985. Developmental constraints and evolution: a perspective from the Mountain Lake conference on development and evolution. *Quarter. Rev. Biol.* 265–287.
- Mayr, E., 1982. *The Growth of Biological Thought: Diversity, Evolution, and Inheritance*. Belknap Pr..
- McCartney, M., Keller, G., Lessios, H., 2000. Dispersal barriers in tropical oceans and speciation in Atlantic and eastern Pacific sea urchins of the genus *Echinometra*. *Mol. Ecol.* 9 (9), 1391–1400.
- Meier, R., 2008. DNA sequences in taxonomy – opportunities and challenges. In: Heled, Q.D. (Ed.), *The New Taxonomy*. CRC Press, Baton Raton, USA, pp. 95–127.
- Mironov, A., 2006. Echinoids from seamounts of the north-eastern Atlantic; onshore/offshore gradients in species distribution. In: *Biogeography of the North Atlantic seamounts*, pp. 96–133.
- Moore, H.B., 1935. A case of hermaphroditism and viviparity in *Echinocardium cordatum*. *J. Mar. Biol. Assoc. Unit. Kingd.* 20 (1), 103–107.
- Moore, H.B., 1936. The biology of *Echinocardium cordatum*. *J. Mar. Biol. Assoc. UK* 20 (3), 655–671.
- Mortensen, T., 1951. *A Monograph of the Echinoidea: Spatangoida*. 2. C.A. Reitzel Publ., Copenhagen.
- Mousadik, A., Petit, R., 1996. Chloroplast DNA phylogeography of the argan tree of Morocco. *Mol. Ecol.* 5 (4), 547–555.
- Müller, K., 2005a. Incorporating information from length-mutational events into phylogenetic analysis. *Mol. Phylogenet. Evol.* 38 (3), 667–676.
- Müller, K., 2005b. SeqState: primer design and sequence statistics for phylogenetic DNA datasets. *Appl. Bioinform.* 4, 65–69.
- Nakamura, Y., 2001. Autoecology of the heart urchin, *Echinocardium cordatum*, in the muddy sediment of the Seto Inland Sea, Japan. *J. Mar. Biolog. Assoc.* 81 (2), 289–297.
- Nunes, C.D.A.P., Jangoux, M., 2004. Reproductive cycle of the spatangoid echinoid *Echinocardium cordatum* (Echinodermata) in the southwestern North Sea. *Invert. Reprod. Develop.* 45 (1), 41–57.
- Nunes, C.D.A.P., Jangoux, M., 2007. Larval growth and perimetamorphosis in the echinoid *Echinocardium cordatum* (Echinodermata): the spatangoid way to become a sea urchin. *Zoomorphology* 126 (2), 103–119.
- Osinga, R., Lewis, W.E., Wopereis, J.L.M., Vriezen, C., Van Duyl, F.C., 1995. Effects of the sea urchin *Echinocardium cordatum* on oxygen uptake and sulfate reduction in experimental benthic systems under increasing organic loading. *Ophelia* 41, 221–236.
- Ouborg, N., Van Treuren, R., Van Damme, J., 1991. The significance of genetic erosion in the process of extinction. II. Morphological variation and fitness components in populations of varying size of *Salvia pratensis* L. and *Scabiosa columbaria* L. *Oecologia*, 359–367.
- Owen, C.L., Messing, C.G., Rouse, G.W., Shivji, M.S., 2009. Using a combined approach to explain the morphological and ecological diversity in *Phanogenia*

- gracilis* Hartlaub, 1893 (Echinodermata: Crinoidea) *sensu lato*: two species or intraspecific variation? *Mar. Biol.* 156, 1517–1529.
- Ozolin'sh, A., Nekrasova, M., 2003. The forming of spatial structure of the soft bottom communities around Furugel'm Island. *Oceanology* 43 (1), 83–90.
- Palumbi, S.R., 1996. What can molecular genetics contribute to marine biogeography? An urchin's tale. *J. Exp. Mar. Biol. Ecol.* 203 (1), 75–92.
- Péquignat, E., 1963. Sur un nouvel *Echinocardium* de Ligurie et de Provence. *Echinocardium fenauxi* n. sp. *Doriana* 3, 138–147.
- Péquignat, E., 1964. Description d'une espèce nouvelle de grande taille, repérée dans trois localités entre Marseille et Gênes: *Echinocardium fenauxi* (Péquignat). *Bull. Inst. Océanograph. Monaco* 62, 1–22.
- Petit, R.J., El Mousadik, A., Pons, O., 1998. Identifying populations for conservation on the basis of genetic markers. *Conserv. Biol.* 12 (4), 844–855.
- Pfenninger, M., Schwenk, K., 2007. Cryptic animal species are homogeneously distributed among taxa and biogeographical regions. *BMC Evol. Biol.* 7, 121.
- Poore, G.C.B., Andreakis, N., 2011. Morphological, molecular and biogeographic evidence support two new species in the *Uroptychus naso* complex (Crustacea: Decapoda: Chirostylidae). *Mol. Phylogenet. Evol.* 60 (1), 152–169.
- Posada, D., 2008. jModelTest: phylogenetic model averaging. *Mol. Biol. Evol.* 25 (7), 1253–1256.
- Posada, D., Buckley, T.R., 2004. Model selection and model averaging in phylogenetics: advantages of Akaike information criterion and Bayesian approaches over likelihood ratio tests. *Syst. Biol.* 53 (5), 793–808.
- Puillandre, N., Cruaud, C., Kantor, Y.I., 2010. Cryptic species in *Gemmuloborsonia* (Gastropoda: Conoidea). *J. Molluscan Stud.* 76 (1), 11.
- Ronquist, F., Huelsenbeck, J.P., 2003. MrBayes 3: Bayesian phylogenetic inference under mixed models. *Bioinformatics* 19 (12), 1572–1574.
- Rosenberg, R., Agrenius, S., Hellman, B., Nilsson, H.C., Norling, K., 2002. Recovery of marine benthic habitats and fauna in a Swedish fjord following improved oxygen conditions. *Mar. Ecol. Prog. Ser.* 234, 43–53.
- Ross, K.G., Gotzek, D., Ascunce, M.S., Shoemaker, D.D., 2010. Species delimitation: a case study in a problematic ant taxon. *Syst. Biol.* 59 (2), 162–184.
- Roux, C., Tsagkogeorga, G., Bierné, N., Galtier, N., 2013. Crossing the species barrier: genomic hotspots of introgression between two highly divergent *Ciona intestinalis* species. *Mol. Biol. Evol.* 30, 1574–1587.
- Rozas, J., Sanchez-DelBarrio, J.C., Messeguer, X., Rozas, R., 2003. DnaSP, DNA polymorphism analyses by the coalescent and other methods. *Bioinformatics* 19 (18), 2496–2497.
- Sáez, A.G., Probert, I., Geisen, M., Quinn, P., Young, J.R., Medlin, L.K., 2003. Pseudocryptic speciation in coccolithophores. *Proc. Natl. Acad. Sci. USA* 100 (12), 7163–7168.
- Saucede, T., Alibert, P., Laurin, B., David, B., 2006. Environmental and ontogenetic constraints on developmental stability in the spatangoid sea urchin *Echinocardium* (Echinoidea). *Biol. J. Linn. Soc.* 88 (2), 165–177.
- Schwarz, G., 1978. Estimating the dimension of a model. *Ann. Stat.* 6 (2), 461–464.
- Schloss, P.D., Gevers, D., Westcott, S.L., 2011. Reducing the effects of PCR amplification and sequencing artifacts on 16S rRNA-based studies. *PLoS ONE* 6 (12), e27310. <http://dx.doi.org/10.1371/journal.pone.0027310>.
- Shanks, A., 2009. Pelagic larval duration and dispersal distance revisited. *Biolog. Bull.* 216 (3), 373.
- Shanks, A., Grantham, B., Carr, M., 2003. Propagule dispersal distance and the size and spacing of marine reserves. *Ecol. Appl.* 13 (sp1), 159–169.
- Simmons, M.P., Müller, K., Norton, A.P., 2007. The relative performance of indel-coding methods in simulations. *Mol. Phylogenet. Evol.* 44 (2), 724–740.
- Simmons, M.P., Ochoterena, H., 2000. Gaps as characters in sequence-based phylogenetic analyses. *Syst. Biol.* 49 (2), 369–381.
- Smith, K.L., Harmon, L.J., Shoo, L.P., Melville, J., 2011. Evidence of constrained phenotypic evolution in a cryptic species complex of agamid lizards. *Evolution* 65 (4), 976–992.
- Stearns, S.C., 1992. *The Evolution of Life Histories*. Oxford University Press, Oxford.
- Stockley, B., Smith, A.B., Liittlewood, T., Lessios, H.A., Mackenzie-Dodds, J.A., 2005. Phylogenetic relationships of spatangoid sea urchins (Echinoidea): taxon sampling density and congruence between morphological and molecular estimates. *Zool. Scr.* 34 (5), 447–468.
- Stöhr, S., Boissin, E., Chenuil, A., 2009. Potential cryptic speciation in Mediterranean populations of *Ophioderma* (Echinodermata: Ophiuroidea). *Zootaxa* 2071, 1–20.
- Strelkov, P., Nikula, R., Väinola, R., 2007. *Macoma balthica* in the White and Barents Seas: properties of a widespread marine hybrid swarm (Mollusca: Bivalvia). *Mol. Ecol.* 16, 4110–4127.
- Thatje, S., Gerdes, D., Rachor, E., 1999. A seafloor crater in the German Bight and its effects on the benthos. *Helgol. Mar. Res.* 53, 36–44.
- Thompson, J.D., Higgins, D.G., Gibson, T.J., 1994. CLUSTAL W: improving the sensitivity of progressive multiple sequence alignment through sequence weighting, position-specific gap penalties and weight matrix choice. *Nucleic Acids Res.* 22 (22), 4673–4680.
- Trontelj, P., Fišer, C., 2009. Cryptic species diversity should not be trivialised. *Syst. Biodivers.* 7 (01), 1–3.
- Vences, M., Thomas, M., Bonett, R.M., Vieites, D.R., 2005. Deciphering amphibian diversity through DNA barcoding: chances and challenges. *Philosoph. Trans. Roy. Soc. B: Biol. Sci.* 360 (1462), 1859–1868.
- Vieites, D.R., Wollenberg, K.C., Andreone, F., Köhler, J., Glaw, F., Vences, M., 2009. Vast underestimation of Madagascar's biodiversity evidenced by an integrative amphibian inventory. *Proc. Natl. Acad. Sci.*
- Vogler, A.P., Monaghan, M.T., 2007. Recent advances in DNA taxonomy. *J. Zool. Systemat. Evolution. Res.* 45 (1), 1–10.
- Vopel, K., Vopel, A., Thistle, D., Hancock, N., 2007. Effects of spatangoid heart urchins on O2 supply into coastal sediment. *Mar. Ecol. Prog. Ser.* 333, 161–171.
- Wada, H., Komatsu, M., Satoh, N., 1996. Mitochondrial rDNA phylogeny of the Asteroidea suggests the primitiveness of the Paxillosida. *Mol. Phylogenet. Evol.* 6 (1), 97–106.
- Wake, D.B., Roth, G., Wake, M.H., 1983. On the problem of stasis in organismal evolution. *J. Theor. Biol.* 101 (2), 211–224.
- Wakeley, J., 2006. *An Introduction to Coalescent Theory*. Roberts and Company Publishers.
- Walsh, P., Metzger, D., Higuchi, R., 1991. Chelex 100 as a medium for simple extraction of DNA for PCR-based typing from forensic material. *Biotechniques* 10 (4), 506–513.
- Wiens, J.J., Graham, C.H., 2005. Niche conservatism: integrating evolution, ecology, and conservation biology. *Annu. Rev. Ecol. Evol. Syst.*, 519–539.
- Williamson, P.G., 1987. Selection or constraint?: a proposal on the mechanism for stasis. In: Campbell, K.S.W., Day, M.F. (Eds.), *Rates of Evolution*. Allen & Unwin, pp. 129–142.
- Wilson, N., Hunter, R., Lockhart, S., Halanych, K., 2007. Multiple lineages and absence of panmixia in the “circumpolar” crinoid *Promachocrinus kerguelensis* from the Atlantic sector of Antarctica. *Mar. Biol.* 152 (4), 895–904.
- Yakovlev, S.N., 1987. Gonad Cycle and Reproduction of the Heart Urchin *Echinocardium cordatum* in the Sea of Japan. *Biol. Morya* 13 (2), 38–43.
- Zhang, D.-X., Hewitt, G.M., 2003. Nuclear DNA analyses in genetic studies of populations: practice, problems and prospects. *Mol. Ecol.* 12, 563–584.
- Zhou, H., Zhang, Z.N., Liu, X.S., Tu, L.H., Yu, Z.S., 2007. Changes in the shelf macrobenthic community over large temporal and spatial scales in the Bohai Sea, China. *J. Mar. Syst.* 67 (3–4), 312–321.